Available online at www.sciencedirect.com
ScienceDirect
Journal of Magnetism and Magnetic Materials 308 (2007) 313–317
Journal of magnetism and magnetic materials
www.elsevier.com/locate/jmmm

Two opposite gradients of hole density in as-grown and annealed (Ga,Mn)As layers

J.J. Deng, J.H. Zhao*, P.H. Tan, J.F. Bi, H.D. Gan, Z.C. Niu, X.G. Wu

State Key Laboratory for Superlattices and Microstructures, Institute of Semiconductors, Chinese Academy of Sciences, P. O. Box 912, Beijing 100083, P R China

Received 9 November 2005; received in revised form 18 May 2006
Available online 5 July 2006

Abstract

The depth distribution of the hole density p in 500 nm-thick (Ga,Mn)As layers is investigated. From Raman scattering spectra, it is found that the gradients of p are opposite in the as-grown and annealed layers. At the region around the free surface, with increasing etching depth, p significantly increases in the as-grown layer; however, p decreases distinctly in the annealed layer. Then, in the bulk, p becomes almost homogeneous for both cases. The etching-depth dependence of Curie temperature obtained from magnetic measurements is in agreement with the distribution characterization of p. These results suggest that annealing induces outdiffusion of Mn interstitials towards the free surface, and incomplete outdiffusion during the growth leads to an accumulation of Mn interstitials around the free surface of the as-grown (Ga,Mn)As.

PACS: 75.50.Pp; 81.40.Rs; 78.30.Fs; 81.15Hi

Keywords: Magnetic semiconductors; Electrical and magnetic properties (related to treatment conditions); Raman spectra; Molecular-beam epitaxy

1. Introduction

The discovery of ferromagnetism in (Ga,Mn)As has paved the way for semiconductor spintronics devices [1]. It is widely accepted that the exchange interaction between itinerant holes and localized magnetic moments leads to ferromagnetism in (Ga,Mn)As [2]. The mean-field theory of Dietl predicted that Curie temperature T_C of (Ga,Mn)As could be enhanced to 300 K by increasing both Mn concentration and hole density p [2]. However, low-temperature molecular-beam epitaxy (LT-MBE) used for growing (Ga,Mn)As is a highly nonequilibrium method, and inevitably induces a high density of defects such as Mn interstitials (Mn_I) and As antisites (As_{Ga}). Both Mn_I and As_{Ga} defects are double donors in (Ga,Mn)As, and therefore compensate a fraction of holes provided by Mn in substitutional sites (Mn_{Ga}). This results in a suppression of T_C [2].

It is known that post-growth annealing at low temperature is an effective method to enhance T_C of (Ga,Mn)As [3–14]. Up till now, T_C of (Ga,Mn)As layers has been enhanced from 110 K to 150–160 K by post-growth annealing [3,7,8]. The obvious enhancement of T_C in (Ga,Mn)As layers is mainly attributed to outdiffusion of Mn_I defects to the free surface of (Ga,Mn)As [3,6]. These Mn_I defects at the surface are passivated by oxidation [3,10], which is responsible for a significant increase of p and T_C of (Ga,Mn)As [12]. This mechanism is supported by GaAs capping-induced suppression and amorphous As capping-induced enhancement of T_C in annealed (Ga,Mn)As layers [6,11,14]. On the other hand, Limmer et al. [13] argued that the increase in p upon post-growth annealing in (Ga,Mn)As layers is not primarily due to outdiffusion of Mn_I. A significant outdiffusion of Mn_I defects occurs only near the surface region, whereas in the bulk, the highly unstable Mn_I defects may rearrange and form electrically inactive randomly distributed precipitates.

To fully understand the inside mechanism for enhancing T_C by post-growth annealing, investigating the depth

*Corresponding author. Tel.: +86 10 8230 4254; fax: +86 10 8230 5056.
E-mail address: jhzhao@red.semi.ac.cn (J.H. Zhao).

0304-8853/$ - see front matter © 2006 Elsevier B.V. All rights reserved.
doi:10.1016/j.jmmm.2006.06.007

distribution of p is very important. It is suggested to be a general phenomenon of (Ga,Mn)As grown by LT-MBE that p monotonically decreases with increasing etching depth d in both as-grown and annealed (Ga,Mn)As layers [13,15]. In this paper, we report the dependence of p upon d in 500 nm-thick (Ga,Mn)As layers. We found that two opposite gradients of p exist in the near-surface region in the as-grown and annealed layers. On the other hand, p becomes almost homogeneous in the bulk for both cases. Our results indicate that annealing induces outdiffusion of Mn_I defects towards the free surface, while an accumulation of Mn_I around the free surface occurs in the as-grown (Ga,Mn)As layers.

2. Experiments

(Ga,Mn)As layers were grown on semi-insulating GaAs (0 0 1) substrates employing a V80MARKI MBE system installed with standard effusion cells containing solid sources of elemental Ga,As and Mn. A 100 nm-thick GaAs buffer layer was first grown at the substrate temperature $T_s = 560\,^{\circ}C$ before the growth of (Ga,Mn)As to smoothen the surface. T_s was then lowered to 250 °C for the growth of (Ga,Mn)As layer. The V/III (As_4/Ga) beam-equivalent pressure ratio was maintained to be 32 and the growth rate was 11 nm/min during the growth. A typical surface reconstruction of (1×2) streaky was kept during and after the growth of (Ga,Mn)As layer, and no sign of the second phase was observed. After growth, one 500 nm-thick (Ga,Mn)As sample with Mn mole concentration of 5.8% was cleaved into six small pieces (samples A–F) for different measurements. The detailed processes of annealing and etching of samples A–F are shown in Table 1. The samples were annealed repeatedly in order to increase T_C and p to the largest possible extent.

To study the p profiling in the as-grown and annealed (Ga,Mn)As layers, we performed Raman-scattering measurements for samples A and B. The micro-Raman spectra were recorded by a Dilor Super Labram system with a typical resolution of 1.0 cm^{-1} in a back-scattering geometry of $\bar{z}(x,y)z$ at room temperature, where $z = [0\,0\,1]$, $x = [1\,0\,0]$ and $y = [0\,1\,0]$. The laser excitation wavelength is 514.5 nm from an Ar^+ laser. Sample A was kept in the as-grown state, and etched by wet-chemical etching using a 3:1:20 (H_3PO_4:H_2O_2:H_2O) solution to different d. Raman-scattering measurement was performed after each run of etching. Sample B was first annealed in air at 270 °C for 1 h, and then etched to different d. Each etching treatment was followed by annealing in air at 270 °C for 1 h to reach the optimum T_C [4,5]. In order to verify the dependence of p upon d obtained from Raman scattering measurements, we performed Hall resistance measurements over a magnetic field range of 0–0.6 T at 300 K with a standard ac transport measurement setup for samples C–E. These three pieces were annealed in air at 270 °C for 1 h. Two of them were etched to the depth 100 nm (sample D) and 200 nm (sample E), and they were then annealed in air at 270 °C for another 1 h.

To investigate the influence of annealing and etching on the magnetic property of (Ga,Mn)As, sample F underwent a series of annealing or etching treatments. The temperature dependence of remanent magnetization M_r of sample F was measured after each run of annealing or etching by superconducting quantum interference device (SQUID).

3. Results and discussions

Fig. 1 shows Raman spectra of sample A with different d. As shown in Fig. 1, the Raman spectrum of a reference sample of undoped GaAs only shows a longitudinal-optical (LO) mode. This is in agreement with the Raman selection rule for a zincblende crystal, where the LO phonon is allowed and the transverse-optical (TO) phonon is forbidden. The Raman spectra of as-grown (Ga,Mn)As layer with different d exhibit a broad peak around TO-frequency region of undoped GaAs with a peak shoulder at its high-energy side. The strong broad peak is the coupled plasmon–LO-phonon (CPLO) mode due to the high carrier concentration in (Ga,Mn)As, and the weak shoulder is the unscreened LO (ULO) phonon mode in (Ga,Mn)As [13]. The relative intensity of the ULO mode to CPLO mode increases with increasing d up to 150 nm, then remains almost unchanged when d exceeds 150 nm. Fig. 2 shows Raman spectra of sample B, which was treated with a series of annealing or etching mentioned above. One can see from Fig. 2 that the CPLO mode frequency and width significantly decrease after sample B was annealed at 270 °C for 1 h. Then, the CPLO mode frequency and width

Table 1
The detailed processes of annealing and etching of samples A–F

Sample series	Initial state	1st run d (nm)	1st run annealing	2nd run d (nm)	2nd run annealing	3rd run d (nm)	3rd run annealing	4th run d (mn)	4th run annealing
A	As-grown	50	No	100	No	150	No	200	No
B	As-grown	0	Yes	100	Yes	200	Yes	—	—
C	As-grown	0	Yes	—	—	—	—	—	—
D	As-grown	0	Yes	100	Yes	—	—	—	—
E	As-grown	0	Yes	200	Yes	—	—	—	—
F	As-grown	0	Yes	25	Yes	100	Yes	200	Yes

Note: d denotes the etching depth.

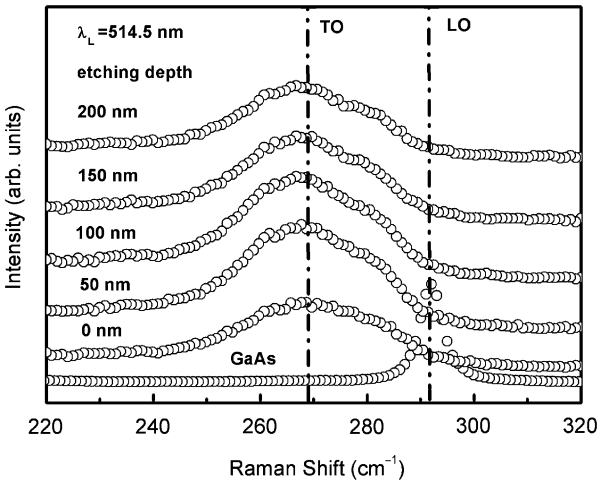

Fig. 1. Raman scattering spectra of the as-grown 500 nm-thick (Ga,Mn)As layer (sample A) corresponding to different etching depths *d*.

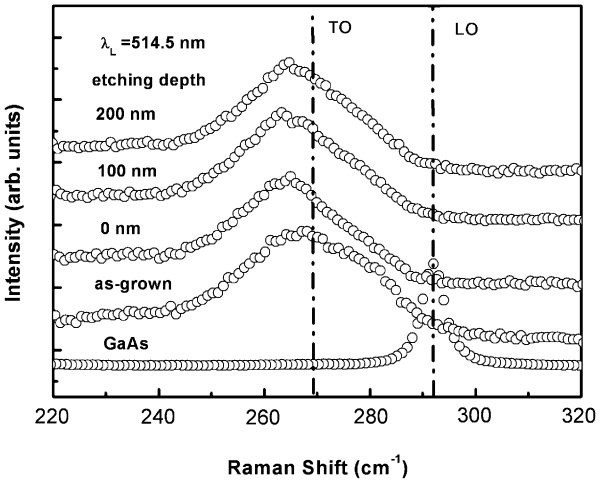

Fig. 2. Raman scattering spectra of the annealed 500 nm-thick (Ga,Mn)As layer (sample B) corresponding to different etching depths *d* with an annealing process at 270 °C in air for 1 h before each run of etching process.

increase after sample B was etched by 100 nm. When *d* is larger than 100 nm, the spectral feature of the CPLO and ULO modes keeps almost unchanged even if sample B experienced further etching or annealing. It should be noted that the light-penetration depth is about 100 nm for the 514-nm laser line, whereas the light-penetration depth is only about 50 nm for the 458-nm laser line. Therefore, the relative strength of the signal arising from the depletion layer is larger for the 458-nm laser line, the LO-phonon mode can be well separated from the CPLO mode [16]. However, the LO-phonon mode cannot be well separated from the CPLO mode for the 514-nm laser line. Consequently, the Raman line shapes shown in Figs. 1 and 2 are similar to the Raman line shapes observed by Koeder et al. [15], but different from that shown in Refs. [13,16], where the 458-nm laser line was used.

The hole density in (Ga,Mn)As can be determined using a Raman-scattering intensity analysis of the CPLO and ULO modes [17]. The calculated dependence of p upon d of samples A and B is summarized in Fig. 3. It is found that two opposite gradients of p exist at the near-surface region in the as-grown and annealed layers. In the as-grown layer (sample A), with increasing d to 150 nm, p significantly increases from 3.1×10^{19} to $1.0 \times 10^{20}\,\mathrm{cm}^{-3}$, then keeps this value when d exceeds 150 nm. However, in the annealed layer (sample B), p decreases distinctly from 2.3×10^{20} to $1.0 \times 10^{20}\,\mathrm{cm}^{-3}$ with increasing d to 100 nm. When d exceeds 100 nm, p remains about $1.0 \times 10^{20}\,\mathrm{cm}^{-3}$ even if sample B experienced further etching and annealing treatments.

The Hall effect is commonly used to measure the concentration of charge carriers in semiconductors. However, a precise determination of p was difficult to obtain by Hall measurement because of the existence of the anomalous Hall effect (AHE). A conventional way to solve this problem is going to use low temperatures and high magnetic fields (above 20 T) where the magnetization and magnetoresistance saturation make it possible to extract the ordinary Hall coefficient [18,19]. The Hall coefficient continues to change with T above 300 K, which is an indication of the presence of the temperature-dependent AHE [20]. As compared with p obtained at high fields (above 25 T) and low temperatures [19], the error of p obtained at high temperature ($T_C < T < 380$ K) and low magnetic fields (below 0.15 T) is up to 30–40% [20]. All the Hall data in this paper were obtained at room temperature under the low magnetic field (<0.6 T). The values of p of samples C, D and E obtained from magneto-transport measurements are also shown in Fig. 3. We found that the error of the data is about 20% compared with that obtained at room temperature under magnetic field up to 8 T in our system. As shown in Fig. 3, although the uncertainty of p obtained from Raman intensities is up to the value of 10% [17], the distribution of p in the

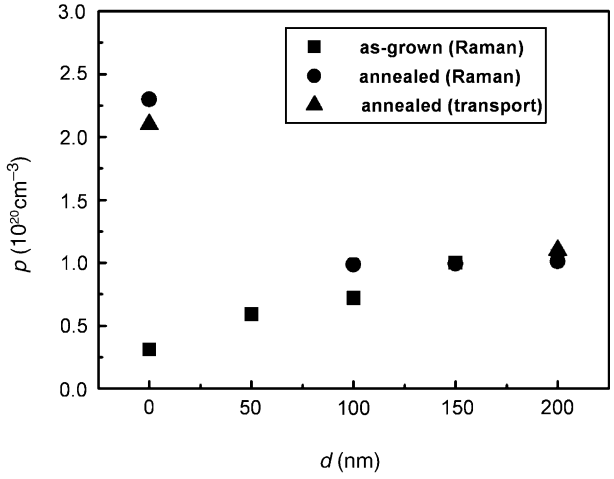

Fig. 3. The depth distribution of p in the as-grown and annealed (Ga,Mn)As layers (samples A and B).

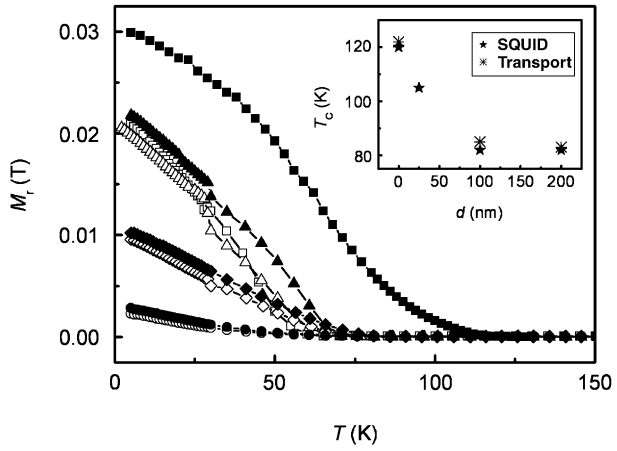

Fig. 4. The temperature dependence of remanent magnetization M_r at zero magnetic field taken from sample F which experienced the following continuous treatment processes: etching to the depths of 0 nm (open squares), 25 nm (open up-triangles), 100 nm (open diamonds), 200 nm (open circles), and the annealing treatments at 270 °C in air for 1 h after each run of etching (corresponding solid symbols), respectively. The inset shows the d dependence of T_C by SQUID and transport measurement techniques.

annealed (Ga,Mn)As layer is consistent with that obtained from Raman spectra patterns on the whole.

One can see from Fig. 4 that T_C of sample F dramatically increases from 63 K (as-grown; open squares) to 120 K (after annealed at 270 °C for 1 h; solid squares). Then, T_C is reduced to 105 K after the 25 nm-thick (Ga,Mn)As was etched off (open up-triangles), and keeps 105 K after the following treatment of annealing at 270 °C for 1 h (solid up-triangles). When d is up to 100 nm, T_C decreases from 105 to 83 K (open diamonds), and then remains 83 K when d exceeds 100 nm even if sample F experienced further annealing or etching treatment (solid diamonds, open circles and solid circles, respectively). Moreover, the value of T_C can also be obtained by using magneto-transport measurements [5]. As shown in the inset of Fig. 4, the values of T_C obtained from SQUID and magneto-transport measurements agree well. For the samples used in the present work, although the Mn concentration is up to 5.8%, the V/III (As_4/Ga) beam equivalent pressure ratio up to 32 could be too high, leading to a lot of As_{Ga}, thus resulting in the low value of p. As is well known, T_C strongly depends on the Mn_{Ga} content x and p ($T_C \alpha xp$) [2]. It is possible that the x is high in these samples, leading to the high T_C.

Unlike the results from other groups, in which p decreases with increasing d in both as-grown and annealed (Ga,Mn)As layers [13,15], our experimental data show that p increases with increasing d at the region near the free surface in the as-grown (Ga,Mn)As layer. It is well known that this property of (Ga,Mn)As is very sensitive to growth conditions such as growth temperature. Furthermore, it is generally assumed that annealing near or even at growth temperature changes Mn_I defects distribution, then this should also inevitably occur during growth of (Ga,Mn)As. In our experiment, during the growth of the 500 nm-thick (Ga,Mn)As layer, Mn_I defects diffuse toward the surface. However, the diffusion rate of Mn_I defects may be lower than the growth rate, which may lead to an accumulation of Mn_I at the region near the surface after growth. This means that compensatory action of Mn_I at the region near the surface is stronger than that inside the bulk. Therefore, p increases with increasing d around the free surface in the as-grown (Ga,Mn)As layer. On the other hand, these accumulated Mn_I defects completely diffuse towards the surface after complete annealing, and finally form a surface oxide layer and do not participate in ferromagnetism of (Ga,Mn)As layer [10]. This results in a significant increase in p around the free surface after post-growth annealing. Since the exchange interaction between local Mn_{Ga} atoms, which is mediated by holes provided by Mn_{Ga}, leads to the ferromagnetism in (Ga,Mn)As [3], the increase in p enhances the ferromagnetic exchange interaction between Mn_{Ga} atoms, and thus increases T_C. This phenomenon indicates that the region near the free surface significantly affects magnetic property of (Ga,Mn)As.

In Fig. 4, we also observe that in the bulk of as-grown or annealed (Ga,Mn)As, T_C is almost unchanged with increasing d, even after further annealing or etching. There are two possible explanations for these observations. First, all the highly unstable Mn_I defects have completely diffused toward the free surface after the first run of annealing at 270 °C for 1 h. Thus, the following annealing after each run of etching scarcely changes the depth distribution of Mn_I defects and p. The second is that a significant outdiffusion of Mn_I defects may happen only in the near-surface region, whereas in the bulk, the highly unstable Mn_I defects rearrange and form electrically inactive randomly distributed precipitates [13]. The implication of this assumption is that p in the bulk is unchanged during annealing after each run of etching. These assumptions are in agreement with the dependence of p upon d obtained from Raman scattering and magneto-transport measurements.

Similar phenomena have been observed in other samples with different Mn concentration after experiencing similar annealing and etching processes mentioned above. Fig. 5 shows the depth distribution of p in the as-grown and annealed 500 nm-thick (Ga,Mn)As layers with Mn mole concentration of 7.6%, deduced by transport measurements. One can see that, similarly, the gradient of p in the as-grown layer is opposite to that in the annealed layer. Moreover, p is lower than that shown in Fig. 3. This may be due to higher Mn_I concentration induced by higher Mn content, compensating a lot of holes provided by substitutional Mn atoms.

On the other hand, from Table 1 one can find that some samples were annealed twice or more than twice. We repeatedly annealed the samples with the deliberate aim to enhance T_C and p to the largest possible extent. However, as shown in Fig. 4, further annealing hardly leads to an increase of T_C and the outdiffusion of Mn_I defects. In

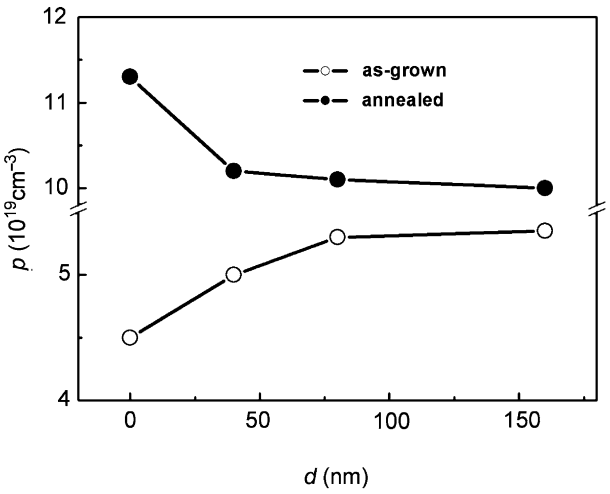

Fig. 5. The depth distribution of p in the as-grown and annealed 500 nm-thick (Ga,Mn)As layers with Mn mole concentration of 7.6%.

addition to that, from Fig. 4, we can also find that etching has no influence on the highly mobile and reactive Mn interstitial defects.

4. Summary

We have observed two opposite gradients of p existing at the region near the free surface in the as-grown and annealed (Ga,Mn)As layers. The p becomes homogenous inside the as-grown and annealed layers. These results suggest that annealing induces outdiffusion of Mn_I towards the free surface and incomplete outdiffusion during the growth results in an accumulation of Mn_I near the surfaces of the as-grown (Ga,Mn)As layers.

Acknowledgements

This work was partly supported by the National Nature Science Foundation of China under Grant no. 10334030 and the special funds for Major State Basic Research Project no. G2001CB3095 of China. The authors thank professors H.Z. Zheng and F.H. Yang for valuable discussions.

References

[1] H. Ohno, A. Shen, F. Matsukura, A. Oiwa, A. Endo, S. Katsumoto, Y. Iye, Appl. Phys. Lett. 69 (1996) 363.
[2] T. Dietl, H. Ohno, F. Matsukura, J. Cibert, D. Ferrand, Science 287 (2000) 1019;
T. Dietl, H. Ohno, F. Matsukura, Phys. Rev. B 63 (2001) 195205.
[3] K.W. Edmonds, P. Boqusawski, K.Y. Wang, R.P. Campion, S.N. Novikov, N.R.S. Farley, B.L. Gallaqher, C.T. Foxon, M. Sawicki, T. Dietl, M. Buonqiorno Nardelli, J. Bernholc, Phys. Rev. Lett. 92 (2004) 037201.
[4] J.J. Deng, J.H. Zhao, C.P. Jiang, Y. Zhang, Z.C. Niu, F.H. Yang, X.G. Wu, H.Z. Zheng, Chin. Phys. Lett. 22 (2005) 466.
[5] C.P. Jiang, J.H. Zhao, J.J. Deng, F.H. Yang, Z.C. Niu, X.G. Wu, H.Z. Zheng, J. Appl. Phys. 97 (2005) 063908.
[6] M. Adell, L. llver, J. Kanski, V. Stanciu, P. Svedlindh, J. Sadowski, J.Z. Domagala, F. Terki, C. Hernandez, S. Charar, Appl. Phys. Lett. 86 (2005) 112501.
[7] D. Chiba, K. Takamura, F. Matsukura, H. Ohno, Appl. Phys. Lett. 82 (2003) 3020.
[8] K.C. Ku, S.J. Potashnik, R.F. Wang, S.H. Chun, P. Schiffer, N. Samarth, M.J. Seong, A. Mascarenhas, E. Johnston-Halperin, R.C. Myers, A.C. Gossard, D.D. Awschalom, Appl. Phys. Lett. 82 (2003) 2302.
[9] T. Hayashi, Y. Hashimoto, S. Katsumoto, Y. Iye, Appl. Phys. Lett. 78 (2001) 1691.
[10] M. Malfait, J. Vanacken, V.V. Moshchalkov, W. Van Roy, G. Borghs, Appl. Phys. Lett. 86 (2005) 132501.
[11] B.J. Kirby, J.A. Borchers, J.J. Rhyne, K.V. O'Donovan, T. Wojtowicz, X. Liu, Z. Ge, S. Shen, J.K. Furdyna, Appl. Phys. Lett. 86 (2005) 072506.
[12] B.S. Sørensen, P.E. Lindelof, J. Sadowski, R. Mathieu, P. Svedlindh, Appl. Phys. Lett. 82 (2003) 2287.
[13] W. Limmer, A. Koeder, S. Frank, V. Avrutin, W. Schoch, R. Sauer, K. Zuem, J. Eisenmenger, P. Ziemann, Phys. Rev. B 71 (2005) 205213.
[14] M.B. Stone, K.C. Ku, S.J. Potashnik, B.L. Sheu, N. Samarth, P. Schiffer, Appl. Phys. Lett. 83 (2003) 4568.
[15] A. Koeder, S. Frank, W. Schoch, V. Avrutin, W. Limmer, K. Thonke, R. Sauer, A. Waag, M. Krieger, K. Zuem, P. Ziemann, S. Brotzmann, H. Bracht, Appl. Phys. Lett. 82 (2003) 3278.
[16] W. Limmer, M. Glunk, S. Mascheck, A. Koeder, D. Klarer, W. Schoch, K. Thonke, R. Sauer, A. Waag, Phys. Rev. B 66 (2002) 205209.
[17] M.J. Seong, S.H. Chun, H.M. Cheong, N. Samarth, A. Mascarenhas, Phys. Rev. B 66 (2002) 033202.
[18] H. Ohno, F. Matsukura, T. Omiya, N. Akiba, J. Appl. Phys. 85 (1999) 4277.
[19] D.V. Baxter, D. Ruzmetov, J. Scherschligt, Y. Sasaki, X. Liu, J.K. Furdyna, C.H. Mielke, Phys. Rev. B 65 (2002) 212407.
[20] D. Ruzmetov, J. Scherschligt, D.V. Baxter, T. Wojtowicz, X. Liu, Y. Sasaki, J.K. Furdyna, K.M. Yu, W. Walukiewicz, Phys. Rev. B 69 (2004) 155207.